

A SIMPLE BOUNDING SURFACE PLASTICITY MODEL FOR SANDS CONSIDERING NON-COAXIALITY OF PRINCIPAL STRESS AND PRINCIPAL PLASTIC STRAIN INCREMENT DIRECTIONS

Ali Lashkari, Azad Islamic University of Shiraz, Shiraz, Iran; also University of Tehran, Tehran, Iran
Manouchehr Latifi, University of Tehran, Tehran, Iran

ABSTRACT

Laboratory tests, using the hollow cylindrical apparatus, demonstrated the deviation between the principal stress and strain increment directions in granular media. This paper presents a state dependent bounding surface plasticity model which able to simulate sand response under loading in hollow cylindrical apparatus during rotation of principal stress directions by using a plastic potential to define the plastic strain increment direction. The model uses a non-associated flow rule and a modified type of plastic modulus, which capable to generate plastic strain in the constant shear stress paths. Model simulations show reasonable agreement with the laboratory tests in the undrained and p-constant drained tests.

1-INTRODUCTION

Experimental studies, using hollow cylindrical apparatus which allows full rotation of principal stress directions, have been shown the significant deviation (sometimes more than 30°) between the principal stress and principal plastic strain increment directions in both loose and dense sands under monotonic and cyclic drained and undrained loadings (Ishihara and Towhata, 1983; Symes et al., 1984; Mura et al., 1986) and Wong and Arthur, 1986).

Many of the constitutive models were formulated based on the results of the tests, which were conducted by fixed principal stress directions. As a result, it is clear that using of such models for loading conditions involving the rotation of principal stress directions can not be recommended.

2-DEFINITIONS

Simulation of sand behavior during the rotation of principal stress directions in the hollow cylindrical apparatus is the aim of the present study. Due to simplicity and performance of many existing experimental data for b=0.5 condition, model was formulated for b=0.5. It must be noted that b is the coefficient of intermediate principal stress and it is defined as:

$$b = \frac{(\sigma_2 - \sigma_3)}{(\sigma_1 - \sigma_3)} \quad [1]$$

where σ_1, σ_2 and σ_3 are the major, intermediate and minor principal stresses, respectively.

Value of b generally varies during the shear in hollow cylindrical apparatus, but as it will be shown later, the assumption of b=0.5 does not affect the model capabilities significantly while this assumption provides low computational efforts.

The model is formulated in the X-Y-p stress space, which is defined as:

$$X = \frac{\sigma_z - \sigma_x}{2} \quad [2-a]$$

$$Y = \sigma_{xz} = \sigma_{zx} \quad [2-b]$$

$$p = \frac{1}{3}(\sigma_x + \sigma_r + \sigma_z) \quad [2-c]$$

where $\sigma_x, \sigma_r, \sigma_z, \sigma_{xz}$ and σ_{zx} are the stress components on specimen in hollow cylindrical apparatus (see Fig.1).

Shear stress in X-Y-p space is simply defined as the projection of the line connecting the origin to the stress state on the X-Y plane and can be calculated by the following equation:

$$\tau = \frac{1}{2}q = (X^2 + Y^2)^{\frac{1}{2}} \quad [3]$$

where, τ is the shear stress and q is the principal deviator stress.

3-GENERAL FORMULATION

According to the elasto-plasticity theory, it is assumed that the total strain increment is the sum of the elastic and plastic strain increments, i.e.

$$\dot{\epsilon} = \dot{\epsilon}^e + \dot{\epsilon}^p \quad [4]$$

Where $\dot{\epsilon}$, $\dot{\epsilon}^e$ and $\dot{\epsilon}^p$ are respectively total, elastic and plastic strain increments. It must be noted that the dot sign over a symbol indicates its rate of change with time.

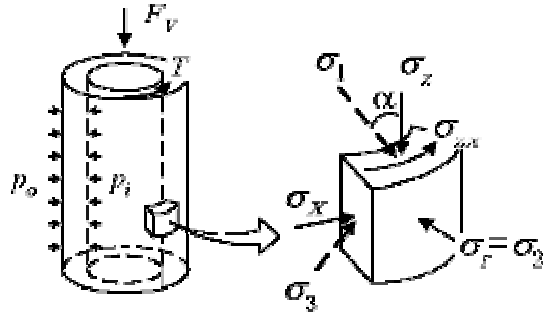


Fig. 1. External forces and stress components on hollow cylindrical specimen (after Yoshimine et al. , 1998)

It is assumed that the elastic part of sand behavior can be completely described by the generalized Hook's law, i.e.

$$\dot{\sigma} = 2G\dot{e}^e + K\dot{\varepsilon}_v^e I \quad [5]$$

Where $\dot{\sigma}$ is the stress increment tensor, e^e and $\varepsilon_v^e I$ are the deviatoric and volumetric parts of the elastic strain tensor respectively. I is the second order isotropic tensor.

G and K are the elastic shear and bulk moduli, that is assumed that are function of overall stress level and some internal material variables like density of the packing.

The elastic shear modulus, G , is calculated using the following empirical equation (Richart et al., 1970):

$$G = G_0 p_{ref} \frac{(2.973 - e)^2}{1 + e} \left(\frac{p}{p_{ref}} \right)^{\frac{1}{2}} \quad [6]$$

Where G_0 is a material constant, p_{ref} is a reference pressure that can be taken as 101 kPa (the atmospheric pressure) and e is the current void ratio.

The elastic bulk modulus, K , can be calculated by the following equation:

$$K = \frac{2}{3} G \frac{(1 + \nu)}{(1 - 2\nu)} \quad [7]$$

Where ν is the poisson's ratio. In the present study it is assumed that the value of ν remains constant during loading.

The plastic strain rate tensor can be calculated by

$$\dot{\varepsilon}^p = \langle \Lambda \rangle R \quad [8]$$

Where R is a tensor defining the direction of plastic strain and Λ is the loading index enclosed by the Macauley

brackets $\langle \cdot \rangle$. Λ can be calculated by the following equation:

$$\Lambda = \frac{1}{K_p} n : \dot{\sigma} \quad [9]$$

Where K_p is the plastic modulus and n is the normal to the yield surface.

4-CONSTITUTIVE SURFACES

According to the concept of Bounding Surface Plasticity (Dafalias & Popov, 1975; Krieg, 1975) and critical state framework, formulation of the model developed.

The model consists of three constitutive surfaces. The first one, called the bounding surface defines all the possible states of stress in the stress space, while the second, called the yield surface, encloses the domain of elasticity in the stress space and the third one is the plastic potential which defines the flow direction, R . Details of each surface is presented in the following.

4-1-BOUNDING (FAILURE) AND YIELD SURFACES

Results of a series of p-constant monotonic drained tests in hollow cylindrical apparatus under the constant b value of 0.5 by Gutierrez et al. (1991) on Toyoura sand, indicated that the failure points defines a circular shape in the X-Y plane (see Fig.2).

As can be seen in Fig.2, due to the inherently anisotropic behavior of sand, the bounding (failure) surface is shifted along the X-direction. Based on experimental observation on Toyoura sand behavior, it is assumed that the Toyoura sand behavior is orthotropic and as a result the bounding surface was not shifted along the Y-direction.

In the present study based on the similar proposition by Gutierrez et al. (1991 and 1993) the following equation is used for the bounding surface.

$$F = \left[\left(\bar{X} - p \frac{\beta}{2} \right)^2 + \bar{Y}^2 \right]^{\frac{1}{2}} - \frac{1}{2} M p = 0 \quad [10]$$

The term of $p \frac{\beta}{2}$ in the above equation, defines the location of the bounding surface center in the X-Y plane.

It is interesting that the same equation as eq.[10] can be obtained by applying the $b=0.5$ condition to the anisotropic type of a Drucker - Prager bounding surface.

Due to the simplicity, a small circular surface is used as the yield surface in the present model. the following equation is proposed for the yield surface in the X-Y plane.

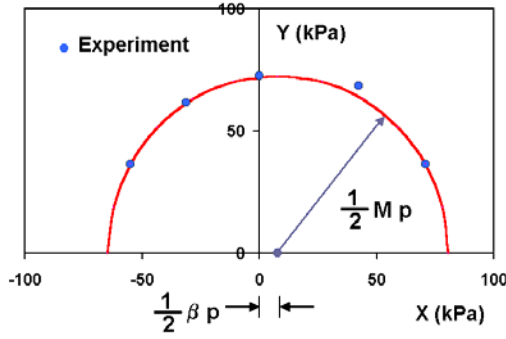


Fig.2 . Failure points from the monotonic p-constant drained tests on Toyoura sand along different fixed principal stress directions (after Gutierrez et al. 1991)

$$f(X, Y, p, \alpha_X, \alpha_Y, m) = \left[(X - p\alpha_X)^2 + (Y - p\alpha_Y)^2 \right]^{\frac{1}{2}} - \frac{1}{2} m p = 0 \quad [11]$$

where $p\alpha_X$ and $p\alpha_Y$ define the location of center of the yield surface in the X-Y plane which can be shifted by anisotropic consolidation or kinematic hardening or both.

4-2-PLASTIC POTENTIAL

Gutierrez et al. (1991) based on experimental results of monotonic and cyclic drained tests by hollow cylindrical apparatus reported that the direction of plastic strain increment is determined as the normal to the failure surface at the point where the extension of the stress increment from the current stress point intersects the failure surface. Some investigators like Gutierrez et al. (1993) and Cubrinovski and Ishihara (1998) formulated their constitutive models using above observation.

In the present study due to the experimental observation suggesting reduction of non-coaxiality of stress and plastic strain increments in drained p-constant tests (Gutierrez et al. ,1990), the plastic potential is permitted to move along the X-axis toward the origin of X-Y plane due to accumulation of plastic shear strain. Besides, in the present study the plastic potential size can be given any other values than the size of the bounding (failure) surface. However, in the simulation of Toyoura sand behavior in the present study, it is assumed that the size of plastic potential is the same as the size of bounding surface.

$$g = \left[(\hat{X} - p \frac{\hat{\beta}}{2})^2 + \hat{Y}^2 \right]^{\frac{1}{2}} - \frac{1}{2} \hat{M} p = 0 \quad [12]$$

where

$$\hat{\beta} = \beta \exp(-f \gamma^p) \quad [13]$$

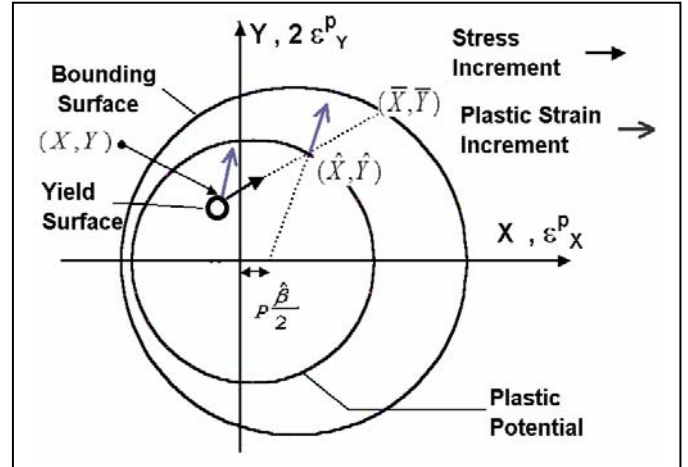


Fig.3 . Yield, bounding and plastic potential surfaces in the X-Y plane with the schematic view of flow rule used in the present study.

In the above equation γ^p is the accumulated plastic shear strain and f is a scalar positive model parameter, which defines the rate of evolution of location of plastic potential center in the X-Y plane. Fig.3 shows the constitutive surfaces in the X-Y plane.

5-YIELD AND FLOW DIRECTIONS

Components of normals to the yield surface and the plastic potential, \mathbf{n} and \mathbf{R} , respectively define the loading and flow directions. They are given by the following equations in the X-Y-p space :

$$n_X = \frac{X - p\alpha_X}{(\frac{mp}{2})} ; n_Y = \frac{Y - p\alpha_Y}{(\frac{mp}{2})} \quad [14-a]$$

$$n_p = \left\{ \alpha_X n_X + \alpha_Y n_Y + \frac{m}{2} \right\} \quad [14-b]$$

$$R_X = \frac{\hat{X} - p \frac{\hat{\beta}}{2}}{(\frac{\hat{M}p}{2})} ; R_Y = \frac{\hat{Y}}{(\frac{\hat{M}p}{2})} \quad [15-a]$$

and

$$R_p = A(\eta_p - nc \eta) \neq n_p \quad [15-b]$$

Above equations imply that a non-associated flow rule exists in the X-Y-p stress space.

R_p , which was called dilatancy coefficient, plays an important role in model simulation. It is observed that the sand behavior, either dilative or contractive, is highly depended on dilatancy coefficient. Considering the stress-dilatancy relationship proposed by Gutierrez et al. (1993)

and Gutierrez and Ishihara (2000) the equation [15-b] was used for the dilatancy coefficient in the present model.

In eq. [15-b], A is a model parameter. η is the stress ratio, η_p is the phase transformation stress ratio that varies as a function of state parameter, ψ , and direction of principal stress direction. In this work, η_p can be calculated by the following equation:

$$\eta_p = \bar{M} \exp(k_d \psi) \quad [16]$$

Where \bar{M} is a parameter defines the size of the bounding surface in each direction. \bar{M} can be defined as the distance of the image of the stress state on the bounding surface from the origin of the X-Y plane.

As it was said before, ψ is state parameter which was defined as $\psi = e - e_c$ by Been and Jefferies (1985). e_c is the value of void ratio on the critical state line, corresponding to the present value of the mean principal effective stress.

Referring to equation [15-b], nc is the non-coaxiality coefficient that defined as below:

$$nc = \cos(2\alpha - 2\omega) \quad [17]$$

Where ω is the angle of principal plastic strain increment direction and it can be calculated by:

$$\tan 2\omega = \frac{\dot{\epsilon}_y^p}{\dot{\epsilon}_x^p} = \frac{\hat{Y}}{\hat{X} - \beta \frac{p}{2}} \quad [18]$$

6-HARDENING RULE

Experimental investigations suggest that the size of elastic zone in normally consolidated sands is very small. Therefore, in the present study the isotropic hardening of the yield surface or the expansion of the yield surface in the stress space is omitted and it is assumed that the yield surface undergoes only the kinematic hardening.

To define the hardening rule, it is necessary to define the mapping rule or the image of the stress state on the bounding surface. The image of any stress state is defined as where the extension of the stress increment in X-Y plane, crosses the bounding surface. In accordance with the Mroz's hardening rule (Mroz, 1967) the instantaneous translation of the yield surface is related to the distance between the stress point and its image on the bounding surface by using a scalar function, ζ .

$$p \dot{\alpha}_X = \zeta \delta_X \quad ; \quad p \dot{\alpha}_Y = \zeta \delta_Y \quad [19]$$

where

$$\delta_X = \bar{X} - X \quad ; \quad \delta_Y = \bar{Y} - Y \quad [20]$$

ζ in the above equations, plays the role of a scaling factor which helps to determine the yield surface translation in the X-Y plane. By imposing the consistency condition to the yield surface:

$$\dot{f} = \frac{\partial f}{\partial X} \dot{X} + \frac{\partial f}{\partial Y} \dot{Y} + \frac{\partial f}{\partial p} \dot{p} + \frac{\partial f}{\partial \alpha_X} \dot{\alpha}_X + \frac{\partial f}{\partial \alpha_Y} \dot{\alpha}_Y = 0 \quad [21]$$

And considering equations [14],[19] and [21], the rate of ζ change can be determined as below:

$$\dot{\zeta} = \frac{n_X \dot{X} + n_Y \dot{Y} + n_p \dot{p}}{n_X \delta_X + n_Y \delta_Y} \quad [22]$$

7-PLASTIC MODULUS

According to equation [9], it is necessary to define the plastic modulus. Based on Li and Dafalias (2000), the following equation was proposed for the present model:

$$K_p = H_0 (1 - H_1 e) G \exp(k_b \psi) \left(\frac{\bar{M} \exp(-k_b \psi) - \eta}{\eta} \right) \times \left(\frac{\bar{M}}{M + \beta} \right)^n \quad [23]$$

Where H_0 , H_1 , k_b and n are the model constants. In above equation H_0 is an initial scalar value modified by the $(1 - H_1 e)$ factor to impose the effect of void ratio on K_p (Li & Dafalias, 2000). Effect of principal stress direction is captured by the last factor to provide the softer response for larger values of α .

8-EXPLICIT FORM OF THE CONSTITUTIVE EQUATIONS

By considering equations [4],[5],[14] and [15] one can has:

$$\dot{X} = 2G\dot{\epsilon}_X = 2G(\dot{\epsilon}_X - \dot{\epsilon}_X^c) = 2G(\dot{\epsilon}_X - \langle \Lambda \rangle R_X) \quad [24-a]$$

$$\dot{Y} = 2G\dot{\epsilon}_Y = 2G(\dot{\epsilon}_Y - \dot{\epsilon}_Y^c) = 2G(\dot{\epsilon}_Y - \langle \Lambda \rangle R_Y) \quad [24-b]$$

$$\dot{p} = K(\dot{\epsilon}_v - \langle \Lambda \rangle R^v) \quad [24-c]$$

knowing from equation [9] that

$$K_p \Lambda = n : \dot{\sigma} = n_X \dot{X} + n_Y \dot{Y} + n_p \dot{p} \quad [25]$$

the loading index is simply calculated as:

$$\Lambda = \frac{n_x \dot{\epsilon}_x + n_y \dot{\epsilon}_y + n_z \frac{K}{2G} \dot{\epsilon}_v}{R_x \cos(2\alpha) + R_y \sin(2\alpha) + \frac{K_p}{2G} + \frac{K}{2G} R_y n_z} \quad [26]$$

9-MODEL PERFORMANCE

The model has been tested for two sets of tests on Toyoura sand. The first set of simulations is conducted for α -constant undrained tests in hollow cylindrical apparatus reported by Yoshimine et al. (1998). The model parameters in the first part of simulations are given in Table.1. As it can be seen in Fig.4, the model is able to predict the response of 5 samples of Toyoura sand with the same densities during the variation of principal stress directions from $\alpha=15'$ to $75'$.

To show that the assumption of $b=0.5$ does not affect the model capabilities significantly, behavior of 6 samples of Toyoura sand in simple shear mode has been simulated (see Fig.5). The model performance is acceptable while the value of b generally varied from 0.5 to 0.25 in failure, as it was reported by Yoshimine et al. (1998).

In the second stage of model evaluation, The model simulations have been compared with the experimental results of p -constant drained, pure rotational stress path tests, conducted by Gutierrez et al.(1991) on dense samples of Toyoura sand with the initial void ratio of 0.711 .

For the tests with $\phi=25'$ and $\phi=30'$ (where $\phi=\sin^{-1}((\sigma_1-\sigma_3)/(\sigma_1+\sigma_3))$), the direction of the principal stresses rotated from 0 to 90 degree while for the test with $\phi=35'$ the principal stress direction were rotated from 15 to 75 degree to prevent the large difference in inner and outer cell pressures. It must be noted that for simulation of behavior in pure rotational stress path tests, the model parameters are the same as those presented in Table.1 except that $M=1.095$, $\beta=0.095$, $H_0=10$ and $n=3$.

Fig.6 shows the comparisons between the experimental in-plane strain components with the model simulations during the rotation of the principal stress direction for the samples with $\phi=25, 30$ and $35'$.

For the same tests, comparisons of measured and predicted values of non-coaxiality during the rotation of principal stress directions are given in Fig.7.

10-CONCLUSION

A relatively simple state dependent bounding surface plasticity model was proposed for modeling the non-

Table 1. Model parameters for Toyoura sand used to simulate the α -constant tests reported by Yoshimine et al. (1998).

Elastic parameters	$G_0 = 125$ $\nu = 0.15$ $m = 0.05 M$
Bounding Surface	$M = 1.225$ $\beta = 0.175$
Plastic Potential	$\hat{M} = 1.225$ $\hat{\beta} = 0.175$ (initial value) $f = 10$
Kinematic Hardening	$H_0 = 2.5$ $H_1 = 1$ $n = 4.0$
State Parameter	$k_d = 3.5$ $k_b = 1.1$
Dilatancy	$A = 0.7$
Critical State Line	$e_c = 0.934 - 0.067\alpha - 0.019 \left(\frac{P}{P_{ref}} \right)^{0.70}$

coaxiality of the principal stress and strain increment directions.

Simulation of sands responses in the hollow cylindrical apparatus under undrained and p -constant drained tests has shown that the model is satisfactory capable to take into account the effects of deviation between the principal stress and strain increment directions.

REFERENCES

- Arthur, J. R. F. & Menzies, B. K. (1972). Inherent anisotropy in sand. *Geotechnique* , Vol. **2** , 419-433.
- Been, K. & Jefferies, M. G. (1985). A state parameter for sands. *Geotechnique* , Vol. **3** , No. 2, 99-112.
- Cubrinovsky, M. & Ishihara, K. (1998). Modeling of soil behavior based on state concept. *Soils Found.* **8** , No. 3, 115-127.
- Dafalias, Y. F. (1986). Bounding surface plasticity, I: Mathematical foundation and hypoplasticity. *J. Engng. Mech.*, ASCE **2** , No. 12, 1263-1291.
- Dafalias, Y. F. & Popov, E. P. (1975). A model of nonlinearly hardening materials for complex loadings. *Acta Mechanica* **2** , 173-192.
- Gutierrez, M., Ishihara, K. & Towhata, I. (1991). Flow theory for sand during rotation of principal stress direction. *Soils Found.* **3** , No. 4, 121-132.

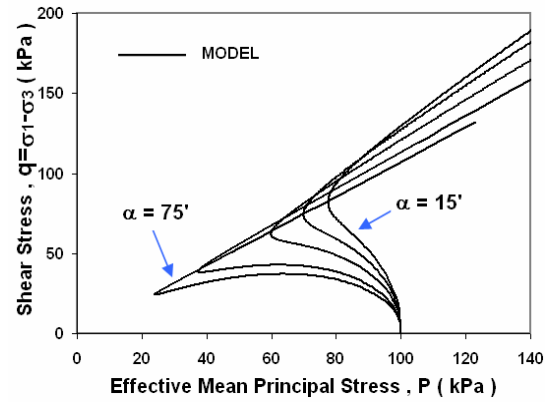
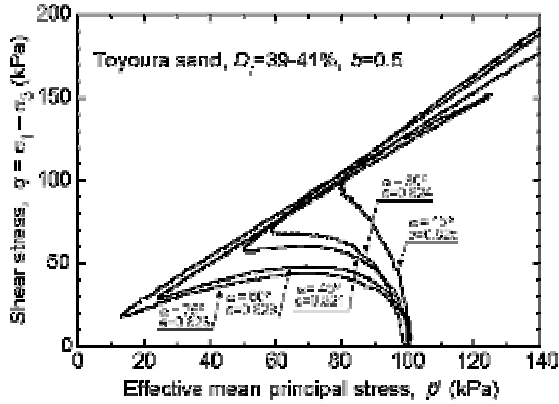
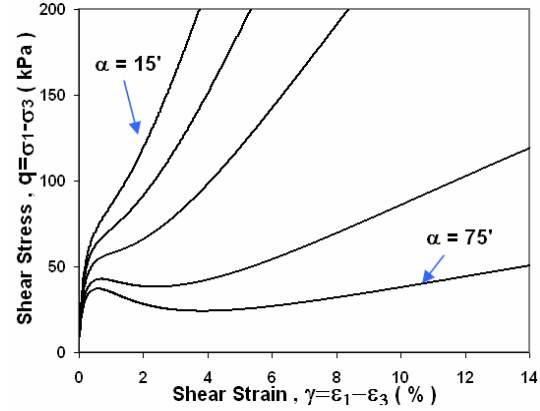
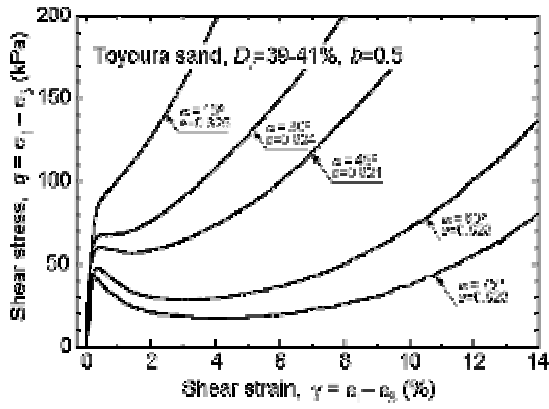


Fig. 4. Comparison of model simulations(Right) with experiments (Left) for influence of principal stress direction on undrained behavior of Toyoura sand

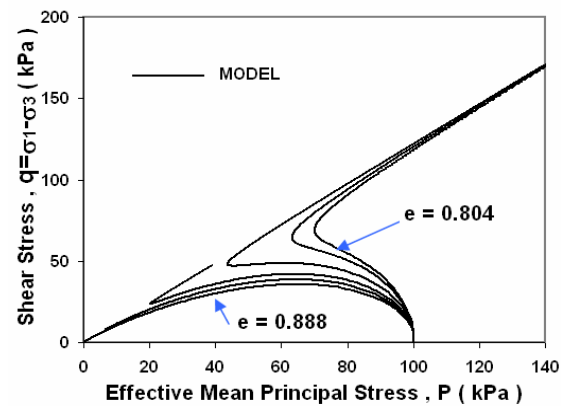
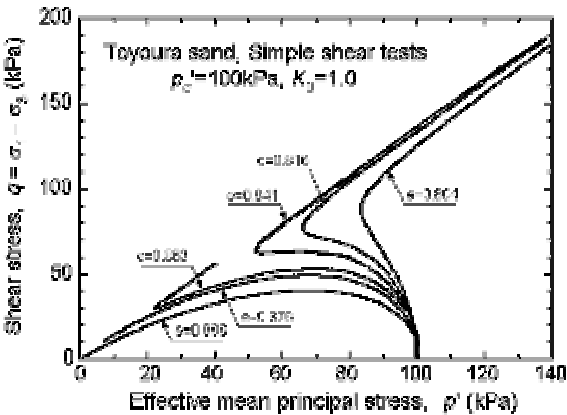
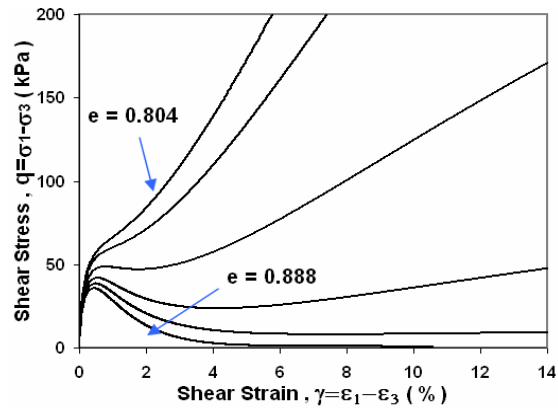
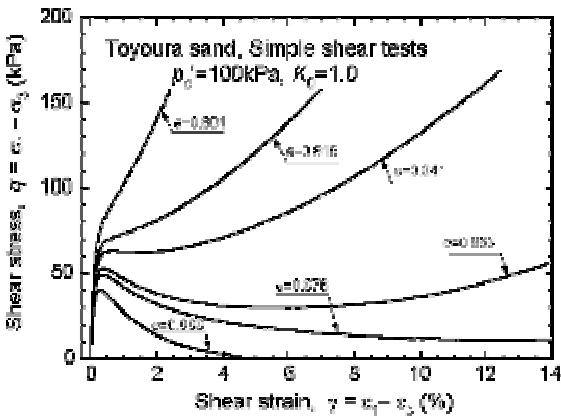


Fig. 5. Comparison of model simulations(Right) with experiments(Left) for isotropic simple shear mode (Data by Yoshimine et al. (1998))

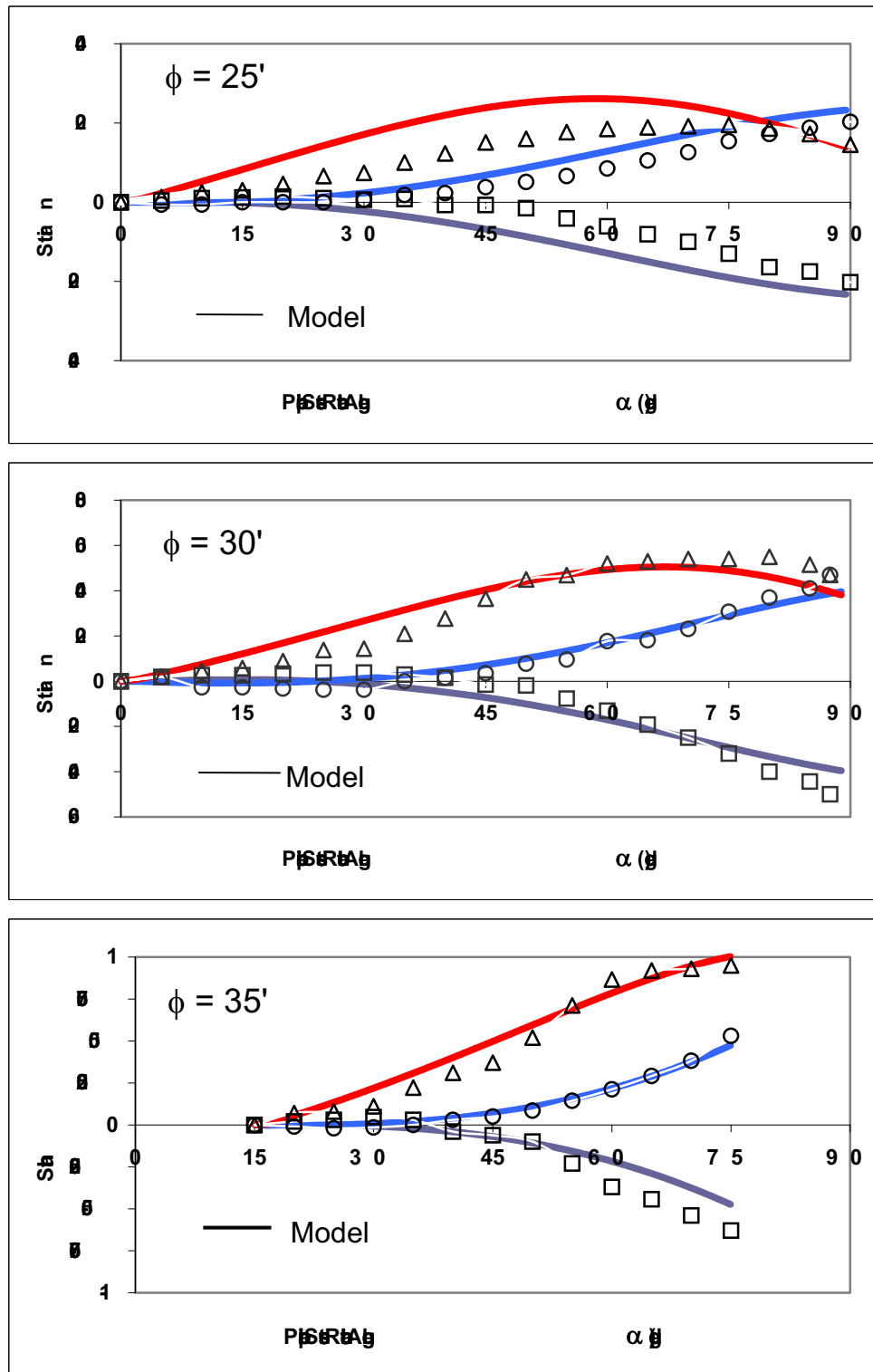


Fig. 6. Comparisons of measured and predicted strains during rotation of principal stress directions for three values of mobilized friction angles: $\phi = 25^\circ$ (top), $\phi = 30^\circ$ (mid), $\phi = 35^\circ$ (but).

Experiment { $\square \epsilon_Z$
 $\circ \epsilon_X$
 $\triangle 2 \epsilon_{ZX}$

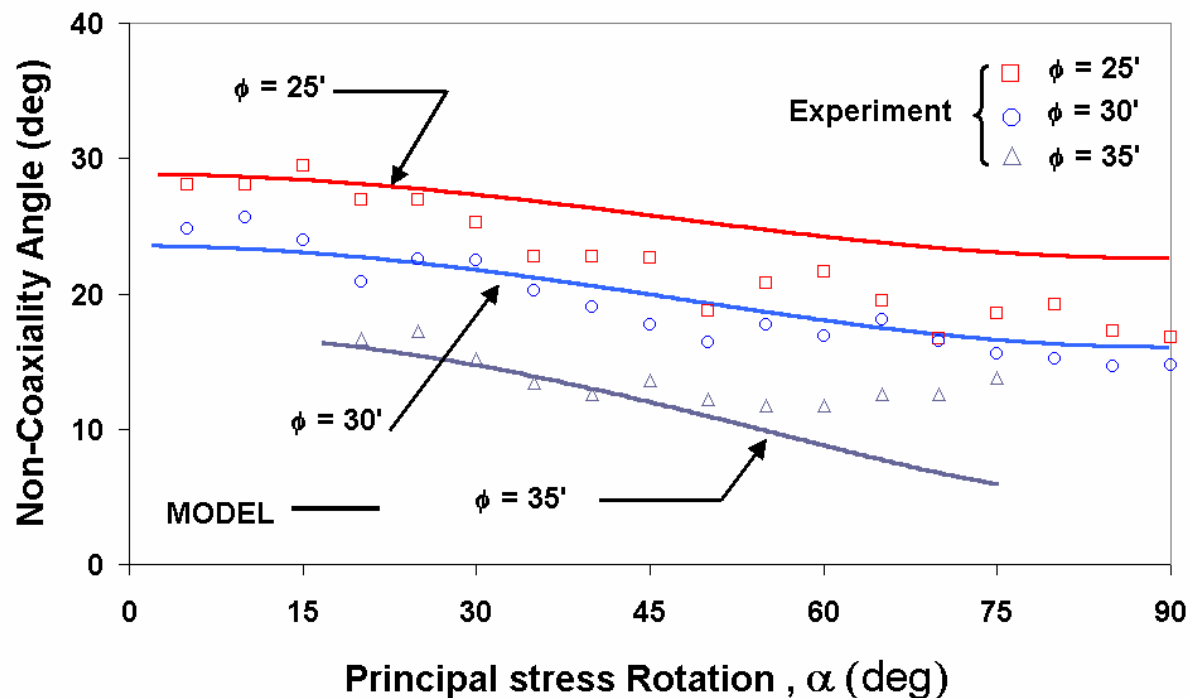


Fig. 7. Comparisons of predicted and measured of non-coaxiality angle, during the rotation of principal stress directions at different constant mobilized friction angles. (Data by Gutierrez et al. (1993))

- Gutierrez, M., Ishihara, K. & Towhata, I. (1993). Model for the deformation of sand during rotation of principal stress directions. *Soils Found.* **3**, No. 3, 105-117.
- Gutierrez, M. & Ishihara, K. (2000). Non-coaxiality and energy dissipation in granular materials. *Soils Found.* **4**, No. 2, 49-59.
- Hight, D. W., Gens, A. & Symes, M. J. (1983). The development of a new hollow cylindrical apparatus for investigating the effects of principal stress rotation in soils. *Geotechnique*, Vol. **3**, No. 1, 11-26.
- Ishihara, K., Towhata, I. (1983). Sand response to cyclic rotation of principal stress directions as induced by wave loadings. *Soils Found.* **3**, No. 4, 105-117.
- Krieg, R. D. (1975). A practical two-surface plasticity theory. *J. Appl. Mech., ASME* **42**, 641-646.
- Li, X. S. & Dafalias, Y. F. (2000). Dilatancy for cohesionless soils. *Geotechnique*, Vol. **50**, No. 4, 449-460.
- Mroz, Z. (1967). On the description of anisotropic work hardening. *J. Mech. And Physics of Solids*, Vol. **15**, 163-175.
- Mura, K., Miura, S. and Toki, S. (1986). Deformation behavior of anisotropic sand under principal axes rotation, *Soils Found.*, Vol. **26**, No. 1, 36-52.
- Nakata, Y., Hyodo, M., Murata, H. & Yasufuku, N. (1998). Flow deformation of sands subjected to principal stress rotation. *Soils Found.* **38**, No. 2, 115-128.
- Oda, M. (1981). Anisotropic strength of cohesionless sands, *ASCE Journal of Geotechnical Engineering Div.*, Vol. **7**, GT9, 1219-1231.
- Richart, F. E. Jr., Hall, J. R. & Wood, R. D. (1970). *Vibration of soils and foundations*. Englewood Cliffs, NJ: Prentice Hall.
- Symes, M. J. P. R., Gens, A. & Hight, D. W. (1984). Undrained anisotropy and principal stress rotation in saturated sand. *Geotechnique*, Vol. **34**, No. 1, 11-27.
- Yoshimine, M., Ishihara, K. & Vargas, W. (1998). Effects of principal stress direction and intermediate stress on undrained shear behavior of sand. *Soils Found.* **38**, No. 3, 179-188.
- Wong, R. K. S. & Arthur, J. R. F. (1986). Sand sheared by stresses with cyclic variation in direction, *Geotechnique*, Vol. **36**, No. 2, 215-226.